Landslides (2014) 11:551–564
DOI 10.1007/s10346-013-0411-7
Received: 4 October 2012
Accepted: 29 April 2013
Published online: 24 May 2013

Jacopo M. Abbruzzese · Vincent Labiouse

New Cadanav methodology for quantitative rock fall hazard assessment and zoning at the local scale

Abstract Rock fall hazard zoning is a challenging yet necessary task to be accomplished for planning an appropriate land use in mountainous areas. Methodologies currently adopted for elaborating zoning maps do not provide satisfactory results though, due to uncertainties and related assumptions characterising hazard assessment. The new Cadanav methodology, presented in this paper, aims at improving quantitative hazard assessment and zoning at the local scale, by reducing uncertainties mainly related to the technique for combining rock fall intensity and frequency of occurrence. Starting from available information on rock fall failure frequency and trajectory simulation results, the procedure merges in a strict way temporal frequency, probability of reach and energy data and evaluates the hazard degree by means of "hazard curves". These curves are described at each point of the slope by a series of energy–return period couples representing the hazardous conditions which may possibly affect that location. The new Cadanav methodology is here detailed and compared to its original version. Hazard zoning results are illustrated along two different 2D slope profiles, for linear homogeneous cliff configurations, and according to the Swiss intensity–frequency diagram for rock fall hazard zoning. However, the procedure can be easily used with any other intensity–frequency diagram prescribed in national guidelines and, additionally, extended to problems involving 3D topographies.

Keywords Rock fall · Hazard · Hazard zoning methodology · Hazard zoning guidelines · Land use planning · Trajectory modelling

Introduction

Urban development in mountainous regions has been significantly increasing in recent years, even in landslide-prone areas. Among the processes which could potentially affect these sites, rock falls represent a major threat for many settlements located at the toe of rocky cliffs. Hazards associated with these phenomena must therefore be properly:

- *assessed*, for quantifying their potential impact on human lives and properties
- *mapped*, for properly regulating land use planning by restricting urban development in hazardous zones, and for designing adequate measures to protect existing endangered urban areas

In the framework for landslide risk management, landslide (e.g. rock fall) hazard can be defined as a condition which may adversely affect human life, property or activity to the extent of causing disasters (Fell et al. 2005; Fell et al. 2008; MR 2010). According to criteria widely accepted at the international level, hazard is completely characterised once the frequency (or probability) of failure of the process, its likelihood of impacting a given location of the slope and its intensity have been evaluated. More specifically concerning rock falls, this means determining the following "hazard descriptors": frequency of detachment of blocks from potentially unstable cliffs, probability that the blocks reach a given point on the slope surface (probability of reach) and kinetic energy along their trajectories. Hazard assessment and zoning maps are therefore meant to provide this type of information.

Currently, plenty of approaches are available for performing rock fall hazard zoning at the local scale (Labiouse and Abbruzzese 2011; Volkwein et al. 2011), either qualitatively (Mazzoccola and Hudson 1996; LCPC 2004; Mölk et al. 2008) or quantitatively (Rouiller et al. 1998; Mazzoccola and Sciesa 2000; Guzzetti and Crosta 2001; Crosta and Agliardi 2003; Jaboyedoff et al. 2005; Desvarreux 2007; Copons 2007; Lan et al. 2007; BLfU 2007). The latest developments in this field of research have been oriented more towards quantitative approaches, mostly based on trajectory modelling results. In principle, quantitative methods provide a sounder and more objective basis for dealing with rock fall problems.

Nevertheless, the majority of the procedures do not provide fully satisfactory results, because of uncertainties affecting the whole process going from the description to the quantification of rock fall hazards. Some of the major issues related to the analysis and management of rock slope instabilities are linked to "model uncertainties" (Einstein et al. 2010). In particular, one important problem is to establish a method for appropriately combining relevant parameters for zoning purposes (i.e. the hazard descriptors mentioned above). More specifically, once rock fall failure frequency has been determined and trajectory simulation data are available, the crucial point is how to merge this information in order to express hazard at a given location on the slope—possibly according to intensity–frequency diagrams, if planned (Raetzo et al. 2002; Altimir et al. 2001).

Issues affecting this methodological aspect suggest therefore the need for further work, aimed at achieving a more rigorous and reproducible zoning practice.

Objective of the research and scope of the paper

The new Cadanav methodology was developed at the Laboratory for Rock Mechanics (LMR) of the École Polytechnique Fédérale de Lausanne (EPFL) with the objective of improving hazard assessment and zoning at the local scale. Its specific goal was to define an objective method for solving the problem presented in the previous section. Starting from data available for the failure frequency, and trajectory simulations results, the new procedure answers the question of how to combine these data and accordingly characterise hazard at any point of the slope.

In this context, the original version of this methodology (Jaboyedoff et al. 2005) attempted already at tackling this point, but strong assumptions were still affecting the results obtained, and constituted somehow a limit for this procedure. New Cadanav was designed to actually remove the main assumptions in the original formulation, in order to provide a more objective approach to zoning.

In line with these purposes, this article recalls the original approach briefly, and then focuses on the detailed presentation of the

new methodology. Comparisons with the original zoning procedure are illustrated along 2D slope profiles for diffuse instability problems potentially affecting linear homogeneous cliffs (i.e. where blocks may detach from any point of a linear rock wall). Benefits and advantages deriving from the application of the new Cadanav procedure are discussed not only in comparison with the original approach, but also with other existing methods.

Original Cadanav methodology

In the context described in the Introduction, the original Cadanav methodology tried to propose a step forward, towards a more objective rock fall hazard zoning based on a quantitative analysis (Jaboyedoff et al. 2005). Established according to the Swiss Guidelines for hazard zoning (Raetzo et al. 2002; Lateltin et al. 2005), important features of this procedure, based on trajectory modelling, are a quantitative consideration of the rock fall failure frequency and the actual combination of energy and frequency for hazard assessment.

According to the original Cadanav methodology (Jaboyedoff et al. 2005), the hazard $\lambda(E,x)$ at a given point x of a slope is expressed as the product between the mean frequency of failure λ_f^* of the rocky cliff, the number of blocks N_{blocks} detaching from the cliff in a single event and the probability of reach $P_r(E,x)$, that is, the probability that a block reaches the selected abscissa x with a given intensity E:

$$\lambda(E,x) = \lambda_f^* \cdot N_{\text{blocks}} \cdot P_r(E,x) \quad (1)$$

Mean failure frequency and size/number of blocks released are estimated starting from historical data on past events, when available (Hungr et al. 1999; Dussauge-Peisser et al. 2002; Hantz et al. 2003; Chau et al. 2003), and a characterisation of the blocks observed on the rock face and on the slope. The distribution of the kinetic energy along the slope is computed by means of rock fall trajectory simulations. For each trajectory, the raw energy profile is modified defining the points x_E where the threshold values E proposed by the Swiss Guidelines (0, 30 and 300 kJ) are reached for the last time, and assigning that energy value to all the points located up-slope. Each profile is basically turned to a step diagram featuring only the three energy values 0, 30 and 300 kJ. Figure 1 (top) illustrates an example of energy profile modification.

Once all the energy profiles have been modified, the abscissas x_E related to a given energy E (e.g. 30 kJ) can be ordered, and the corresponding percentage of blocks travelling beyond each of these abscissas computed. By repeating this procedure for the three thresholds of 0, 30 and 300 kJ, three probability curves can be obtained (Fig. 1, centre), which link the probability of reach at x to a given energy threshold E (Jaboyedoff et al. 2005; Abbruzzese et al. 2009).

The limits of the hazard zones x_{Ei} are given by those abscissas which are passed by one block with an energy higher than E_i, over a specified period of time. For an assigned reference time t_{ref}, the probability of reach associated to this condition is given by:

$$P_r(E_i, x_{Ei}) = \frac{1}{\lambda_f^* \cdot t_{\text{ref}} \cdot N_{\text{blocks}}} \quad (2)$$

The boundaries of the hazard zones x_{Ei} can be determined by using the probability curves in combination with the Swiss intensity–frequency diagram, for seven intensity–frequency couples of

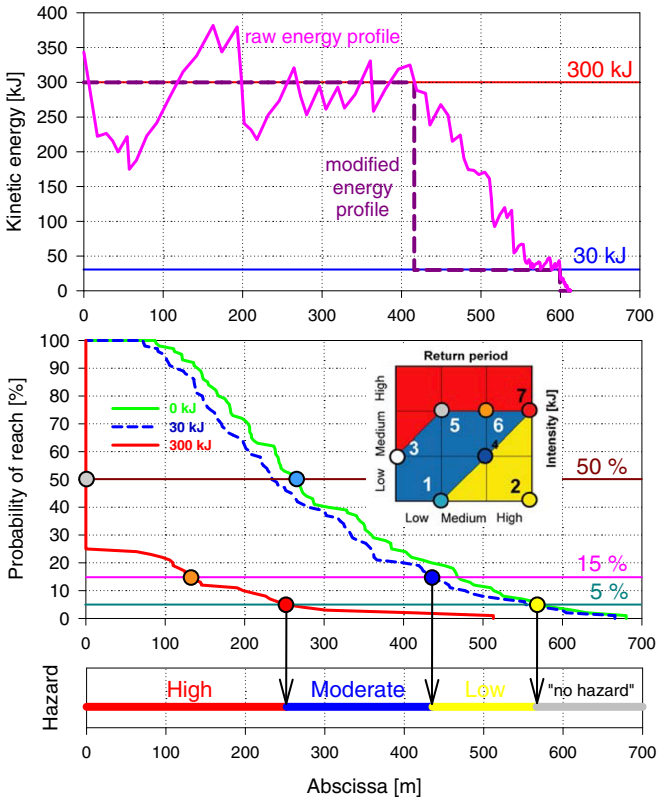

Fig. 1 Hazard zoning according to the original Cadanav methodology. *Top* energy profile modification. *Centre* probability curves and zoning procedure. *Bottom* hazard zoning along a 2D slope profile, for events constituted by five blocks released on average every 75 years (from Labiouse and Abbruzzese 2011)

the diagram (Fig. 1), which mark a change between different hazard levels (points numbered 1 to 7 in Fig. 1, centre).

Each hazard zone limit, i.e. the abscissa beyond which the probability is lower than the calculated value $P_r(E_i,x_{Ei})$, is then established based on the most unfavourable case among the different intensity–frequency couples (i.e. hazardous condition giving the most downhill abscissa). Detailed explanations about the methodology are provided in Labiouse and Abbruzzese (2011).

Limits of original Cadanav

Two strong hypotheses characterise the original Cadanav methodology.

The first involves the trajectory data post-processing, and is constituted by the modification of the energy profiles. This assumption is conservative in terms of hazard level estimation and makes land use applications easier, as it ensures that the hazard level constantly decreases down-slope (Jaboyedoff et al. 2005). On the other hand:

- It may represent a loss of detail concerning the information available about the process and related hazard. Additionally, keeping the raw information on the kinetic energy is useful for considerations involving the design of protection measures and for risk analyses.
- When the energy profiles are modified, the probability a block reaches a given point of the slope with an energy equal or greater than E might be considerably overestimated. This could in turn lead to remarkably overestimate the extent of

the high hazard zone, as well as the extent of the moderate hazard zone, even though with less important effects. This issue happens in fact for "complex" topographies, whose profiles may be characterised by steps, e.g. steep parts followed by flatter zones (where the blocks may possibly come almost to rest before the slope becomes steep again), or more in general by any topographical feature which can strongly alter the distribution of kinetic energy along the slope.

The second assumption is linked to the criterion used for determining the hazard zone limits, according to the Swiss intensity–frequency diagram. In particular, the extent of the hazard zones is established based on the most unfavourable energy–return period conditions obtained by testing only seven combinations in the Swiss intensity–frequency diagram (Fig. 1). This may lead to neglect other energy–return period combinations that might represent more unfavourable conditions and consequently, to underestimate the extent of the hazard zones.

Additionally, it must be remarked that the definition of the failure frequency is quite general, and misses a spatial reference, i.e. a unit length for 2D problems or a unit surface for 3D.

Formulation of the new procedure for hazard zoning

The new procedure, as the original, provides a hazard description expressed in terms of rock fall *frequency of occurrence* λ. It is given by the following equation:

$$\lambda(E,x) = \lambda_f \cdot P_r(E,x) \cdot d \tag{3}$$

expressed in $[\text{years}]^{-1}$, where $\lambda(E,x)$ is the mean frequency of blocks reaching a given slope unit (abscissa x) with an energy higher than an energy threshold E, λ_f is the rock fall frequency of failure (i.e. inverse of the mean failure time T_f), $P_r(E,x)$ the probability of reach associated to the energy value E (i.e. the probability that a block reaches a point x of the slope with an energy higher than E) and d the block size.

The structure of Eq. 3 is based on the equation used in the original approach; however, several new aspects and modifications distinguish the proposed formulation from the previous.

The frequency of failure at the source area is defined as the mean number of blocks of a specific volume potentially detaching from the cliff within a given observation period t_{obs} and per unit length. For diffuse instability problems, in a linear homogeneous cliff configuration, rock falls can be considered as evenly distributed all over the potentially unstable zone (Hantz 2011). Therefore, a failure frequency per linear metre of cliff can be defined, dividing the frequency of events estimated for the whole cliff by its length L. If the potentially unstable compartments are assumed to be characterised by the same volume and to release blocks of a certain volume, the frequency of block released per linear metre of cliff λ_f is given by:

$$\lambda_f = \frac{N_{ev} \cdot N_{blocks}}{t_{obs}} \cdot \frac{1}{L} \tag{4}$$

expressed in [years • m^{-1}] where N_{ev} is the number of events (i.e. compartment failures) occurring within the observation time t_{obs} and N_{blocks} the mean number of fragments released in each event—which can be determined, e.g. based on the discontinuity patterns of the rock mass at the source area, or, in order to account for fragmentation, by combining the information at the source area with the volume of the blocks observed in the propagation zone (Corominas et al. 2005). When compared to the less-detailed definition given for λ_f^* in the original Cadanav methodology, it can be noticed that the failure frequency λ_f to be considered for hazard zoning is now formulated in terms of mean number of blocks released in a given time frame, and is specified with reference to the length of cliff actually releasing blocks in the underlying run-out area. With respect to original Cadanav, a relation between the two expressions for the failure frequency can be therefore written as: $\lambda_f = N_{blocks} \bullet \lambda_f^* / L$.

The probability of reach is computed at each point of the slope in relation to a specific energy level E, though the considered energy values are not anymore only those representing the thresholds in an intensity–frequency diagram (i.e. 0, 30 and 300 kJ in the Swiss Codes), but all those found at the point considered.

Additionally, Eq. 3 takes into account the fact that the probability for a point of the slope to be reached by a block depends not only on the path of the block on the slope surface, but also on the size d of the block (e.g. equivalent block diameter, or maximum side length for rectangular prism-shaped blocks), as shown in the scheme in Fig. 2.

When the block size is considered, the trace a trajectory marks on the slope surface is not simply a "line" described by the block's centre of mass (Fig. 2a), but a strip of width d (Fig. 2b and c). Therefore, a point of the slope at a given location will be hit not only when it lays on the trace of the block's centre of mass (Fig. 2a, point 1), but also at any position within the strip of width d (positions 2 and 3 in Fig. 2b and c).

Once the failure frequency has been defined and the trajectories have been computed with a rock fall simulation program, the new Cadanav procedure allows for combining the failure frequency with the propagation and the intensity of the process as follows.

At first, all the energy values found at a given abscissa x as a result of the trajectory simulations are used for building a cumulative distribution curve (Fig. 3).

For each energy value E, the obtained E–$P(E,x)$ energy–probability curve defines the percentage of blocks found at the abscissa x considered with an energy equal or lower. For instance, referring to Fig. 3, 80 % of the blocks reach the selected abscissa with an energy lower or equal to 300 kJ

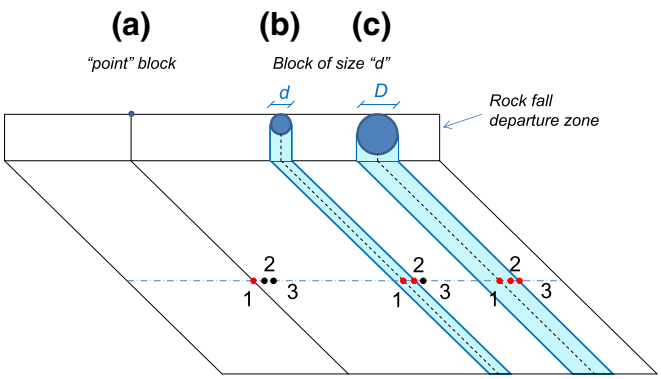

Fig. 2 Influence of the block size d on the section of slope affected by a rock fall trajectory, and on the estimation of the frequency of occurrence. *Red marks* the considered point of the slope is hit by the block, *black marks* the point is not hit

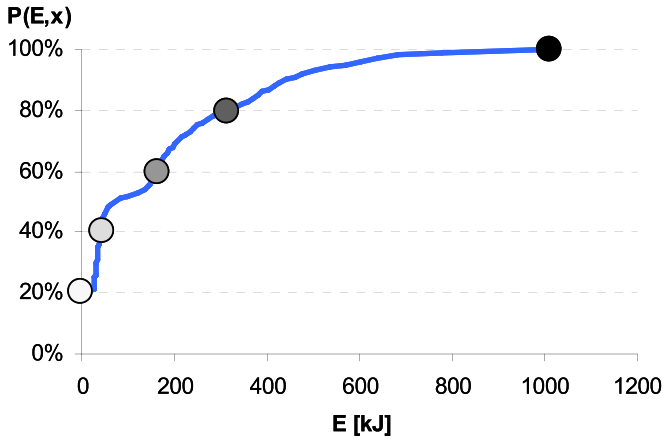

Fig. 3 First step of the new Cadanav methodology: construction of the cumulative energy–probability curve E–$P(E,x)$ at a given abscissa x

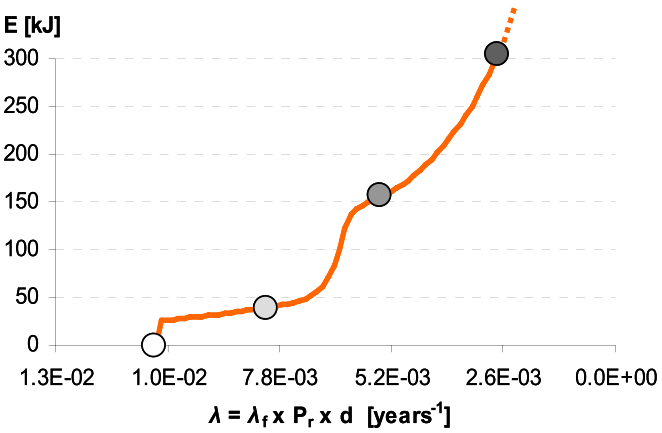

Fig. 5 Third step of the new Cadanav methodology: energy–frequency of occurrence distribution obtained by combining probability of reach $P_r(E,x)$ and failure frequency λ_f

(dark grey point). This percentage, computed over the total number of trajectory runs, also includes blocks which may have possibly stopped before that abscissa. The curve in Fig. 3 shows therefore a probability of 6 % in correspondence of the graph origin, i.e. 6 % of the blocks stopped up-slope.

The second step is to compute the probability that a block reaches the considered abscissa with an energy higher than E, i.e. the probability of reach $P_r(E,x)$. It is given by the value complementary to the previously calculated $P(E,x)$:

$$P_r(E,x) = 1 - P(E,x) \tag{5}$$

where $P(E,x)$ is defined in [0, 1] and, consequently, $P_r(E,x)$ in [1, 0] (Fig. 4).

The failure frequency and the probabilities of reach associated to each energy level are combined in the third step of the methodology according to Eq. 3, so that a distribution of frequency of occurrence–energy couples is obtained at the point considered (Fig. 5).

In the fourth step, the information in terms of frequency of occurrence is translated in terms of return period T, for expressing the hazard in terms of energy and return period.

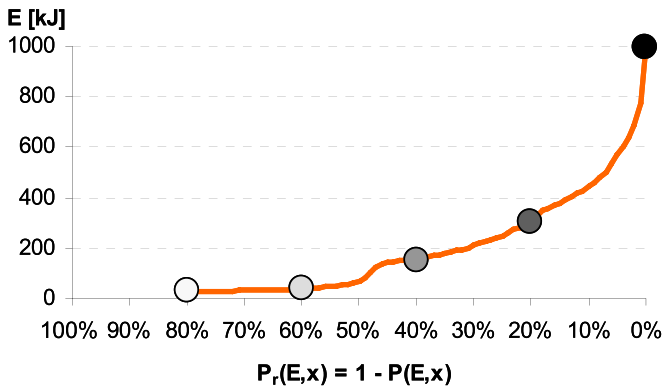

Fig. 4 Second step of the new Cadanav methodology: construction of the probability of reach curve $P_r(E,x)$–E from the cumulative energy curve E–$P(E,x)$

Since the relationship between frequency λ and return period T is $\lambda = 1/T$, by inverting Eq. 3 it results:

$$T(E,x) = \frac{1}{\lambda(E,x)} = \frac{1}{\lambda_f \cdot P_r(E,x) \cdot d} = \frac{T_f}{P_r(E,x) \cdot d} \tag{6}$$

In this equation, T is expressed in [years] and T_f is the return period of blocks released referred to a linear metre of cliff:

$$T_f = \frac{1}{\lambda_f} = \frac{t_{obs} \cdot L}{N_{ev} \cdot N_{blocks}} \tag{7}$$

and therefore expressed in [years • m]. As λ_f is the inverse of T_f, it is worthwhile to point out here that, if the reference length considered in Eqs. 4 and 7 is e.g. doubled, the failure frequency λ_f will be reduced by a factor 2 while, accordingly, T_f will be multiplied by a factor 2.

The new procedure allows therefore for quantitatively describing hazard in terms of occurrence time within which a block detaching from a cliff every T_f years on average reaches a point x with an energy higher than E. In particular, from the energy–frequency of occurrence curve E–$\lambda(E,x)$, an energy–return period curve E–$T(E,x)$ called "hazard curve" can be derived (Fig. 6).

When the hazard level is planned to be assessed based on an intensity–frequency diagram established in guidelines (e.g. Swiss Codes), the hazard curve can be superimposed to such a diagram for determining the degree of hazard affecting a given point of the slope (Fig. 7). In this fifth and last step, according to the location of the E–T couples on the diagram, the hazard degree can be assessed based on the following criterion:

- If the hazard curve is entirely contained in one single domain of the diagram corresponding to a given hazard level, the considered slope unit is assigned that hazard level.
- If the curve crosses more than one hazard domain, the hazard degree is established based on the most unfavourable case.

Figure 7 shows a hazard curve superimposed on the Swiss diagram, represented in two apparently different shapes. The

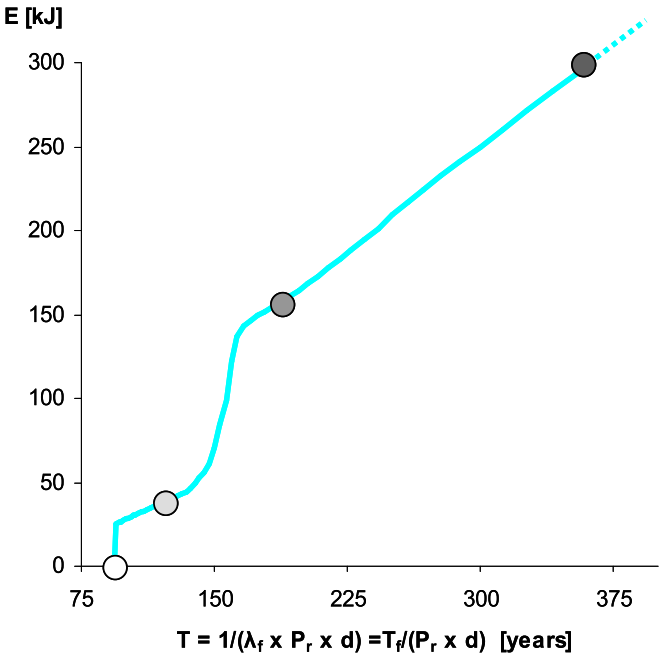

Fig. 6 Fourth step of the new Cadanav methodology: construction of the energy–return period curve E–$T(E,x)$, hereafter called as "hazard curve"

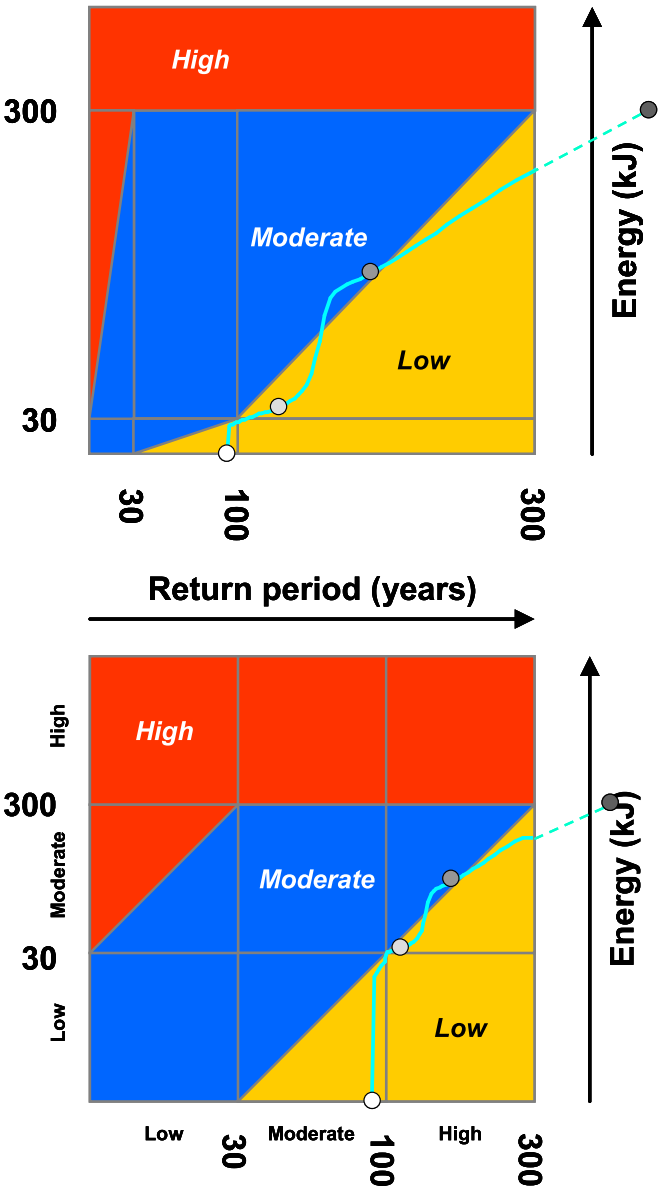

Fig. 7 Fifth step of the new Cadanav methodology: overlapping of the hazard curve to the Swiss intensity–frequency diagram. *Top* diagram represented in linear scale. *Bottom* usual representation used in the Swiss Codes

lower matrix is the one used in the Swiss Codes (Raetzo et al. 2002). The upper matrix illustrates the diagram represented in linear scale. This scaling was assumed for axes and diagonals, in order to perform "numerically" the overlapping between the hazard curve and the matrix, since the Swiss recommendations do not give any information about this.

In terms of implications on land use planning, degrees of hazard and associated colours correspond to the following measures. In high hazard areas (red zone) any new building and development of existing urban areas are forbidden. Moderate hazard (blue zone) means new buildings in new urban areas are forbidden, but further development of existing ones are allowed under conditions (e.g. protection measures). Low hazard areas (yellow zone) can on the other hand be built or developed with minor or no restrictions.

By repeating the procedure at each slope unit, the hazard degree can be determined all over the study site. A schematic example of application of the new Cadanav methodology for a 2D slope profile is given in Fig. 8, which illustrates how hazard curves allow for assessing the hazard level at each location of the slope. Moving from the source area towards the toe (e.g. from point A to point C), it can be observed how the curves tend to move towards the low right corner of the diagram, i.e. the hazard degree decreases as expected at increasing distances from the rock fall source areas.

Comparison between the original and new Cadanav procedures

In this section, the new Cadanav procedure is compared with the original version at two sites situated in the Canton of Valais, in Switzerland (Fig. 9).

For each site, a homogeneous linear cliff configuration was assumed, and one profile was selected as a reference topographic model for the hazard analysis. The profile at Creux de Chippis is characterised by a regular slope, whereas the profile selected at Zeneggen is marked by a sequence of steep and flat zones.

Concerning the evaluation of the failure frequency, as the following applications have the academic purpose of testing the new methodology against the original in different scenarios and topographic configurations, the selected values constitute assumptions, and therefore may not necessarily reflect the real conditions found on site.

Hazard zoning for a regular 2D slope profile

Study area

The first comparison was carried out along a 2D slope profile of the Creux de Chippis site (Fig. 9). This profile is taken as an example of "regular" topography, because of its quite uniform

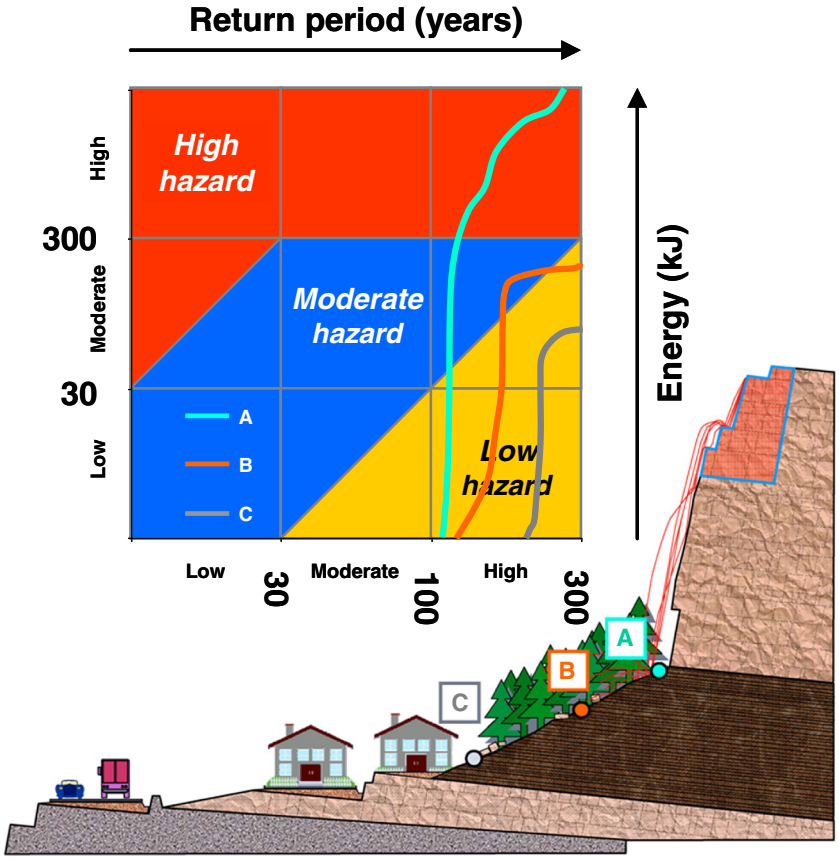

Fig. 8 Schematic example of the new Cadanav methodology: hazard evolution along the slope as described by hazard curves. High hazard at point A (*cyan curve*); moderate hazard at point B (*orange curve*); low hazard at point C (*gray curve*)

slope, not presenting any significant singularity (Fig. 10). Dolomitic limestone and Triassic gypsum constitute the cliffs of this area, which are characterised by three main discontinuity sets. The slope profile selected is identified as P2, and starts at an altitude of 900 m, ending at 550 m. From the source area down to an altitude of about 600 m the slope surface is constituted by rock outcrops and scree deposits. More downhill, the outcropping material is constituted by soil covered by blocks. A road is located approximately at the "boundary" of these two areas at an altitude of about 600 m.

Data analysis and simulation

Rock fall simulation results were provided by the geological firm Géoval, performing 10,000 trajectories. The computations were run with the Rockfall 6.0 code (Spang and Krauter 2001), and the number of trajectories considered is in line with the considerations developed in Abbruzzese et al. (2009). The appropriate block sizes were defined based on the results of detailed field observations of the rock walls. The block volume was estimated equal to 0.5 m^3 and a size of 1 m was considered as the most relevant for the hazard analyses (e.g. parallelepiped-shaped block, with side dimensions of 1×1×0.5 m).

Three failure frequency scenarios were assumed, represented by one event of one block falling on average every 10, 30 and 75 years per linear metre of cliff, respectively.

Results

Figure 10 illustrates for the T_f=10 years·m scenario how the zoning can be obtained all along the profile, as a result of the assessment provided by the hazard curves used in the new Cadanav methodology. At the bottom of this figure, hazard curves are reported for three points *A*, *B* and *C*, located at x=350 m, x=380 m and x=440 m, respectively.

At point A the hazard curve crosses the moderate and high hazard domains of the Swiss matrix, which means that this point must be assigned a high hazard, according to the criterion explained in the previous section. In the same way, at point B the curve crosses the moderate and low hazard domains, which corresponds to a moderate hazard at this location. Finally, for point C, the whole curve is contained in the low hazard part of the diagram: the hazard at the corresponding abscissa is low.

With regards to the hazard curve at point C, it is worthwhile to point out why the new methodology can provide a low hazard when the return period at the source area is lower than 30 years m (as in this example, for T_f=10 years·m), i.e. when the curve is supposed to start in the moderate hazard area. Actually, as 90 % of the blocks do not reach point C, i.e. 10 % of the blocks travel farther down-slope, $P_r(E=0\ \text{kJ})=0.1$ and Eq. 6 yields an initial return period value $T(0\ \text{kJ}, 440\ \text{m})=T_f/0.1=100$ years—which is where the curve starts along the x-axis of the diagram.

For the assumed failure frequency scenario, the high (red), moderate (blue) and low (yellow) hazard zone limits are located at

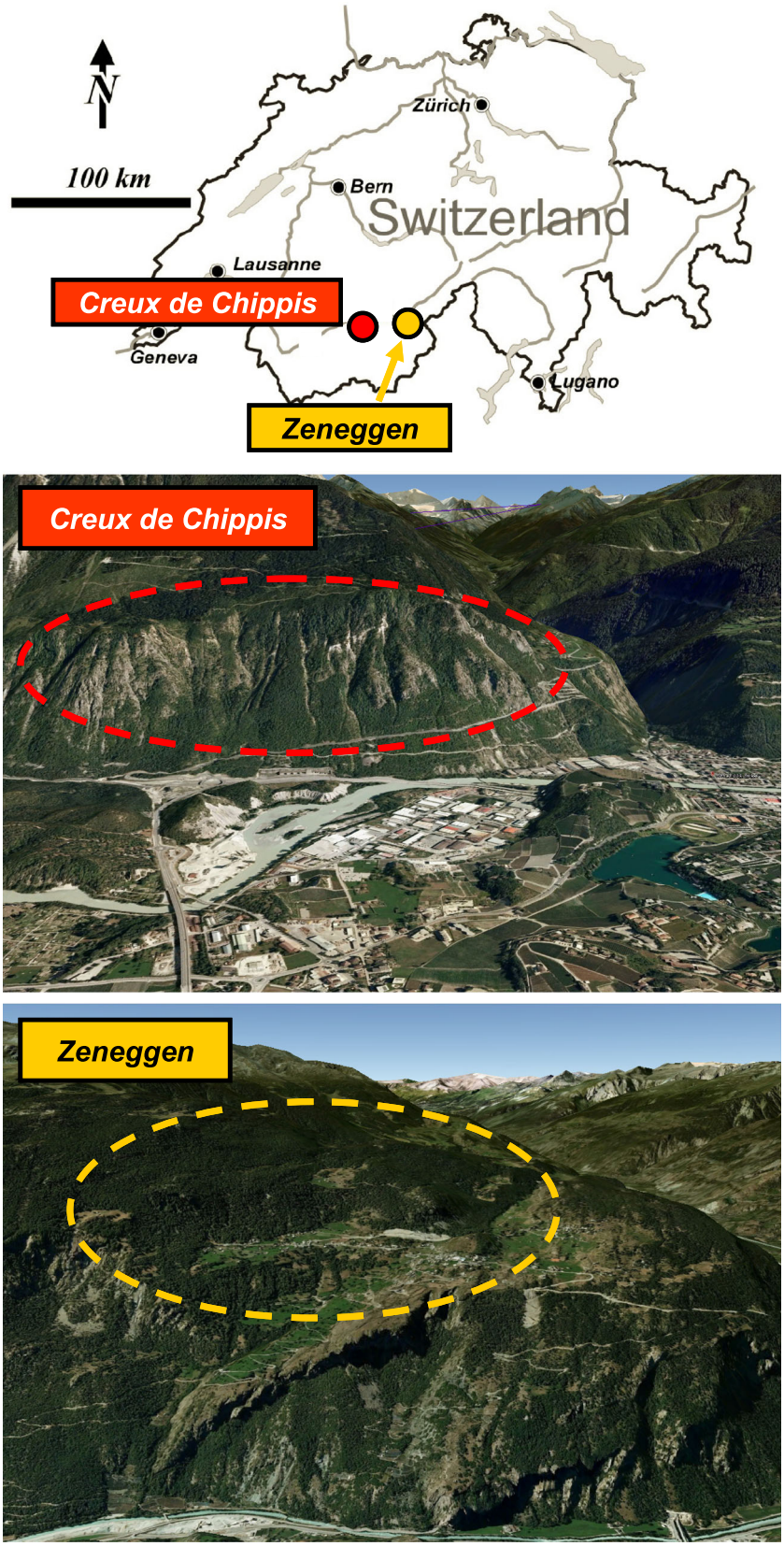

Fig. 9 Location of the study sites of Creux de Chippis and Zeneggen, Canton of Valais, Switzerland (sources: Jaboyedoff et al. 2005; Google Earth)

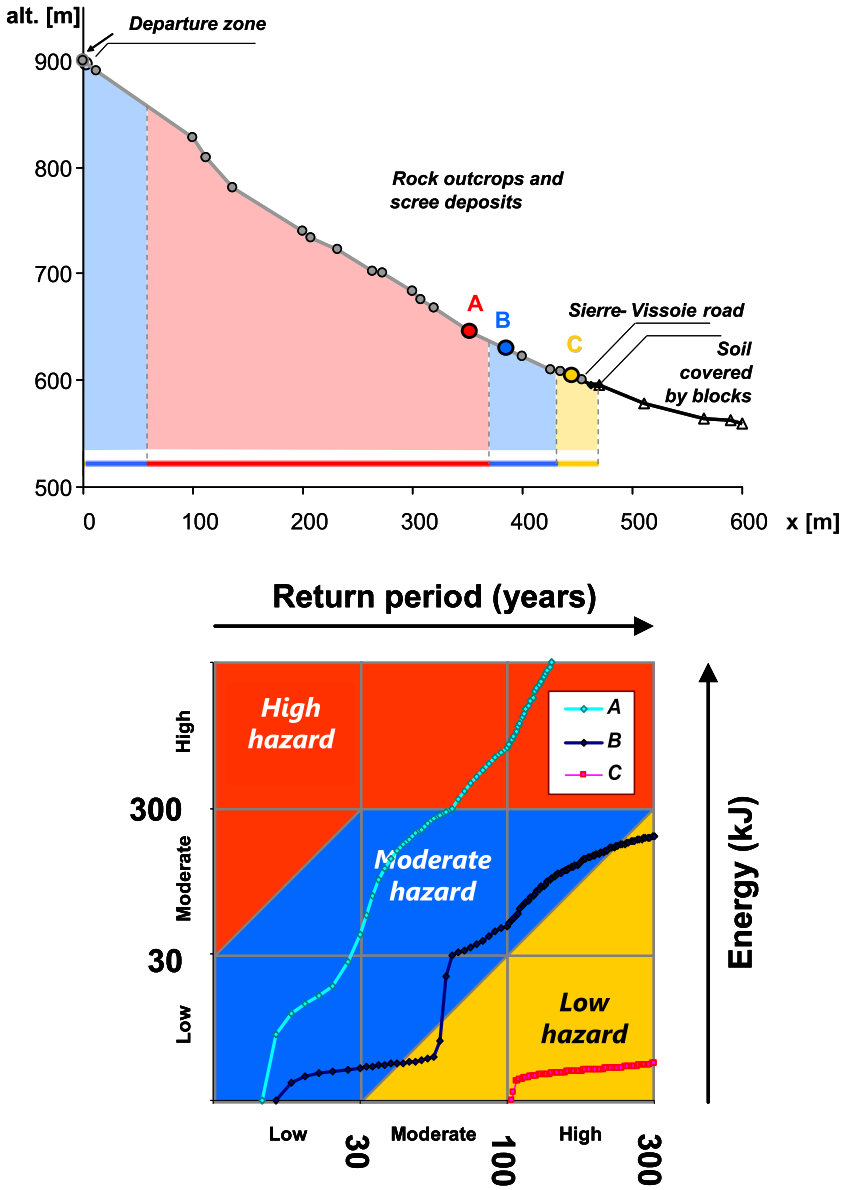

Fig. 10 Hazard zoning according to the new Cadanav methodology along the P2 Profile of Creux de Chippis, for a block volume of 0.5 m^3 and a return period of 10 years • m. The hazard curves reported for points *A*, *B* and *C* show how hazard evolves down-slope

x=370 m, x=430 m and x=467 m, respectively. In terms of land use, any new construction or development would be forbidden up to x=370 m, allowed under major restrictions (including protection measures) up to x=430 m, and only minor restrictions would apply to new constructions and development up to x=467 m.

Looking at the results presented in Fig. 11 for the three failure frequency scenarios considered, a very good general agreement can be observed between the zoning provided by the original (bottom line in each graph, marked as "O") and the new methodology (top lines, marked as "N"). The limits of the low, moderate and high hazard zones match quite well, or even perfectly, in some cases. This can be related to the fact that the probability curves built after modifying the energy profiles in the original Cadanav have quite a similar shape with respect to the raw probability of reach curves obtained from the rock fall simulation and used in the new methodology.

A perfect match of the results can be observed when analysing the position of the low hazard zone limit. This happens because no modification of the energy profile is actually required in the original Cadanav procedure, for building the o kJ probability curve. It is in fact equal to the raw probability curve and consequently, the extent of the low hazard zone is the same according to both methodologies, for all the tested failure frequency scenarios.

Concerning the moderate hazard zone, also the position of the boundary of this area is the same, for λ_f=1/10 and λ_f=1/30 $(\text{years}\cdot\text{m})^{-1}$. In contrast, for λ_f=1/75 $(\text{years}\cdot\text{m})^{-1}$ the original Cadanav does not provide any moderate hazard zone (details about the occurrence of this issue are given in the Discussion section).

On the other side, slightly more important differences in Fig. 11 concern the extent of the high hazard zone, always larger according to

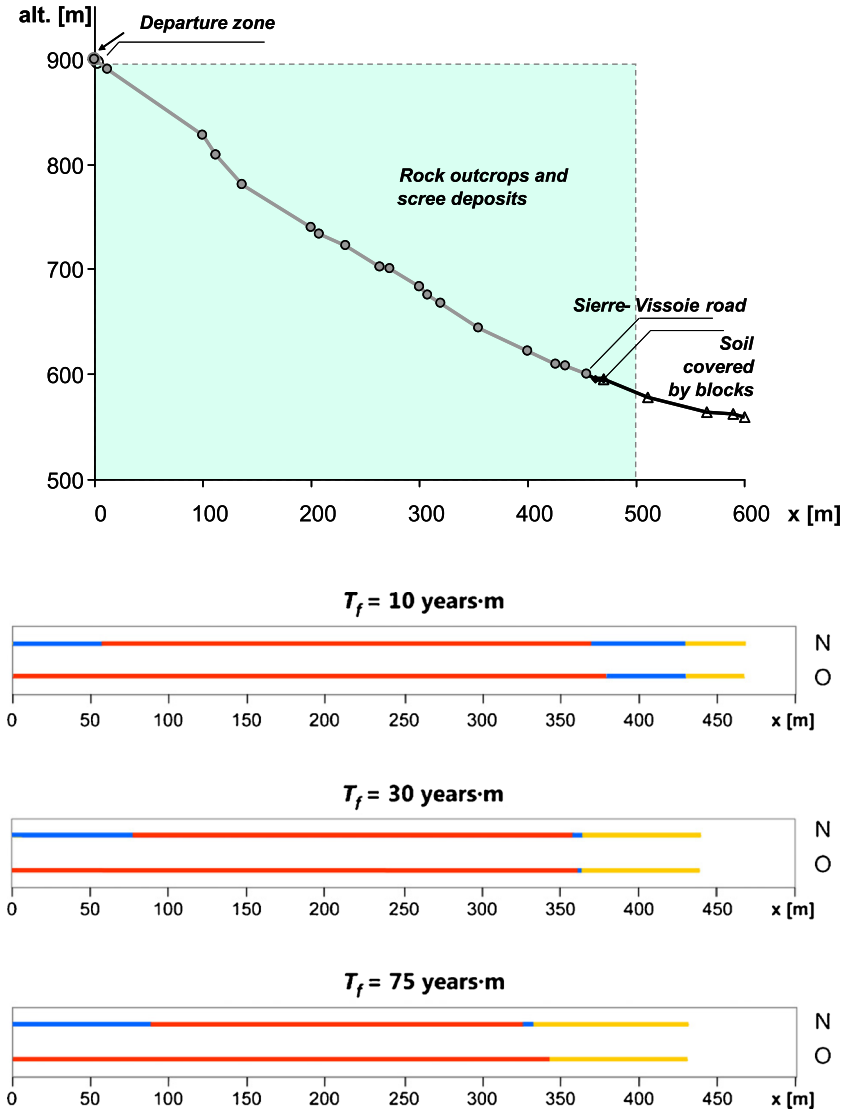

	high hazard	*mod. hazard*	*low hazard*
T_f = 10 years·m			
New	370	430	467
Original	380	430	467
T_f = 30 years·m			
New	359	364	439
Original	362	364	439
T_f = 75 years·m			
New	326	332	430
Original	343	-	430

Fig. 11 Hazard zoning obtained from the original (*O*) and new (*N*) Cadanav methodologies at Creux de Chippis—P2 Profile, for a 0.5-m^3 block volume, according to the Swiss Codes. The results are reported for return periods of the events T_f equal to 10, 30 and 75 years • m

the original approach, and are of 10 and 17 m for failure frequencies of 1/10 and 1/75 (years·m)$^{-1}$, respectively. These differences are due to the tendency to overestimating the probability of reach in the original Cadanav.

Another point that can be noticed is that the new methodology provides a moderate hazard zone in the initial part of the profile, close to the source area. Indeed, although this area is in fact crossed by a large number of blocks (i.e. high frequency of occurrence), their energy is not yet high enough to yield a high degree of hazard.

Globally, the maps obtained suggest the preliminary conclusion that hazard analyses performed along "regular"

topographic profiles, provide a good match between the results obtained from the two procedures. These results somewhat constitute a validation of the approach used in the new methodology with respect to the original. On the contrary, the next section gives an example of the issues that can be observed when comparing the hazard zoning obtained from the two methodologies along an "irregular" slope profile.

Hazard zoning for a complex 2D slope profile

Study area

The original and new Cadanav methodologies were applied at the site of Zeneggen (Fig. 9), performing the zoning for a slope profile identified as P1. In contrast with the former profile, this one can be considered as "irregular", as mentioned previously, due to a more marked sequence of steep and flat zones. The area is essentially characterised by hard rocks of gneiss and mica, featuring five main discontinuity sets, and the profile selected is located between 1,600 and 1,350 m of altitude (Fig. 12, top). The slope surface is constituted by scree deposits, from the source area (1,600 m) down to about 1,430 m, and then soil covered by blocks, down to an altitude of 1,400 m. Farther down-slope, the surface is mainly characterised by the presence of soft soil.

Data analysis and simulation

The hazard zoning was also based on 10,000 trajectory runs provided by the geological firm Géoval, and the block volume considered is 2 m^3, with a size d of 2 m (adopting a parallelepiped shape of 2.0×1.0×1.0 m). As mentioned before, the original Cadanav procedure does not explicitly account for the block size in the hazard assessment (Eq. 1). In order to have a description of hazard comparable with the one provided by the new procedure, therefore, Eq. 1 was multiplied by d.

As in the previous application, three failure frequency scenarios were assumed, equal to one event of one block every 20, 60 and 150 years per linear metre of cliff. These values were considered for the purpose of comparing the two methodologies, and do not necessarily represent conditions on site.

Results

Figure 12 shows how much the results obtained for a complex topography can vary according to the methodology applied. The first point that can be noticed is that the original version of Cadanav confirms to yield a more "conservative" zoning, i.e. a larger extent of the high and moderate hazard zones.

The differences observed in the high hazard zone extent for failure frequencies of 1/60 and 1/150 $(\text{years}\cdot\text{m})^{-1}$ are considerable, i.e. of 83 and 92 m, respectively.

This gives a clear view of how much important the consequences of modifying the energy profiles in the original Cadanav can be.

With regards to the moderate hazard zone, there are also discrepancies, but less important, for frequencies of 1/20 and 1/60 $(\text{years}\cdot\text{m})^{-1}$: 19 and 3 m, respectively. In contrast, for λ_f=1/150$(\text{years}\cdot\text{m})^{-1}$, original Cadanav does not predict any moderate hazard zone.

The second point that can be observed is that the new Cadanav can account for "inverse zoning", i.e. lower hazard zones located before higher hazard zones. Such a complex sequence of zones results in fact from removing the energy profiles modification. In these conditions, the probability of reach values $P_r(E,x)$ reflect the variability of the raw energy values obtained along the slope, and so the frequency of occurrence $\lambda(E,x)$ given by Eq. 3 does. If the objective of the energy profiles modification in the original methodology was also to avoid inverse zoning, as recalled previously, accounting for it can on the other hand allow for sounder decisions for land use planning based on a more rigorous zoning. Referring to Fig. 12, the delineation of a high hazard zone up to x=133 m for T_f=20 years·m, as given by original Cadanav, might be quite unfavourable, knowing that the new approach predicts in fact a moderate hazard zone between x=60 and x=120 m, approximately. As explained by Lateltin et al. (2005), according to the Swiss Codes such a space could be destined to some development, instead of being totally forbidden. The same happens for the area located between x=40 and x=135 m, for T_f=150 years·m, characterised by a sequence of low and moderate hazard zones. Even in case such a sequence should be ignored, and a decision for land use be taken based simply on the most unfavourable condition in this area, a moderate hazard would result from the new methodology. On the contrary, the original methodology would predict a high hazard. Following the Swiss Codes, therefore, some development would indeed be allowed according to the new methodology, even though under restrictions, while the original procedure would yield again a total prohibition domain.

The new procedure allows therefore obtaining a rigorous and detailed hazard assessment along complex slope topographies, where on the contrary the original Cadanav cannot provide a fully satisfying description of hazard, due to its limitations.

Comparison of hazard zoning for other case studies

Comparison analyses as those illustrated above were carried out also for other slope profiles, block volumes and failure frequency values. These tests were aimed at investigating whether the preliminary conclusions drawn for the selected examples of regular and complex topographies could be generalised (Abbruzzese 2011). Indeed, this is the case, and it was observed that a good match in the results is normally obtained when hazard zoning is performed along regular profiles, while significant differences, possibly including inverse zoning, may characterise the zoning maps elaborated for more complex topographies. With regards to irregular topographies, discrepancies in the extent of the high and moderate hazard zones are likely to vary a lot, and their importance may range from small (or even null) to considerable. In the worst cases, hazard zones predicted by one methodology are not predicted by the other. For instance, the moderate hazard zone might be missing in either the original or in the new procedure, or the high hazard zone might be missing in the new procedure while it is predicted by the original.

In most cases, it is confirmed that the original Cadanav provides a more conservative zoning, i.e. high and moderate hazard zones larger than those provided by the new methodology. However, results in contrast with this trend can be noticed in a few cases. This can be explained by keeping in mind that also the second hypothesis characterising the original Cadanav influences hazard zoning, and must be accounted for when comparing the results of the two procedures. More precisely, using only a limited number of energy–return period couples for hazard degree assessment (Fig. 1) could leave out of consideration other couples along the diagonals of the diagram which might be relevant for

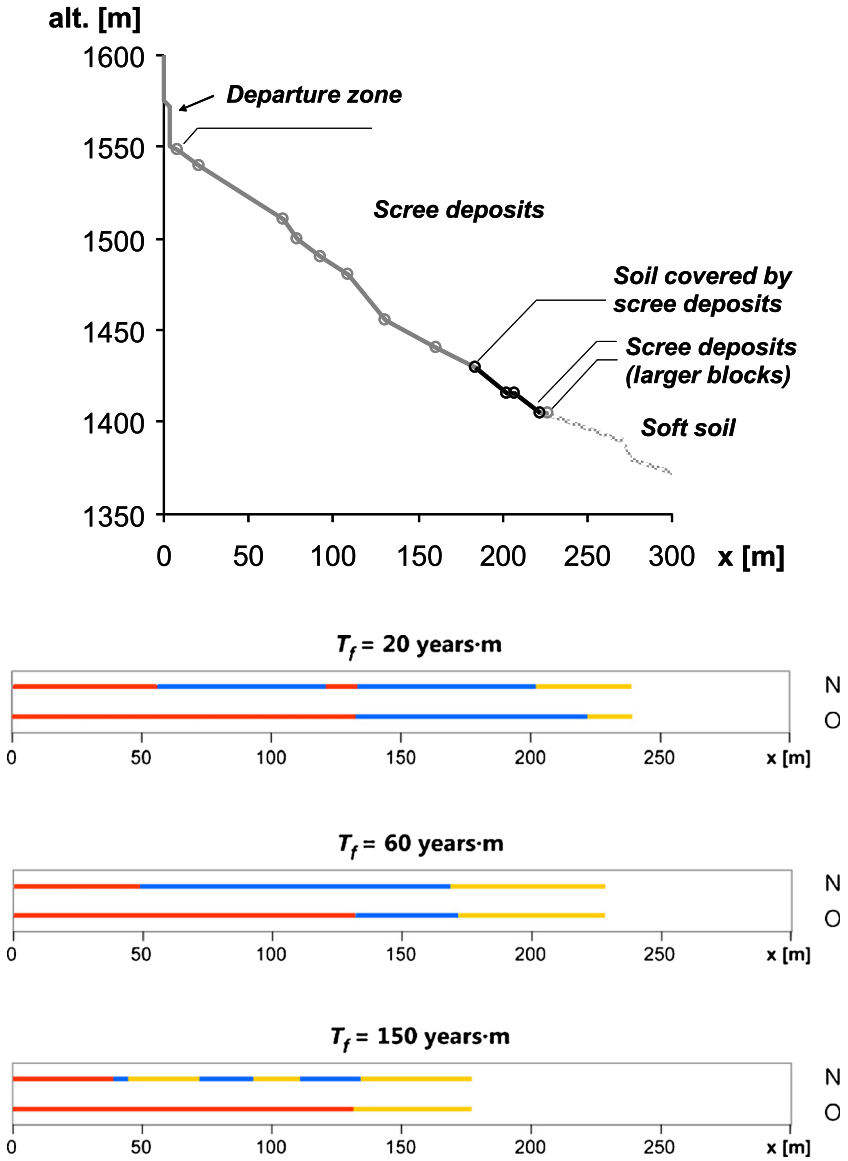

	high hazard	*mod. hazard*	*low hazard*
T_f = 20 years·m			
New	133	203	238
Original	133	222	238
T_f = 60 years·m			
New	49	169	227
Original	132	172	227
T_f = 150 years·m			
New	40	135	176
Original	132	-	176

Fig. 12 Hazard zoning obtained from the original (*O*) and new (*N*) Cadanav methodologies at Zeneggen—P1 Profile, for a 2-m^3 block volume, according to the Swiss Codes. When inverse zoning occurs, only the boundary of the last hazard zone in the sequence is reported in the table, for each hazard degree. The results are reported for values of the return period of the events T_f equal to 20, 60 and 150 years • m

determining the extent of the areas affected by high or moderate hazard. This means that the extent of these zones could be underestimated by the original methodology, as new energy–return period couples could constitute more unfavourable conditions with respect to those originally tested.

Discussion

Further assessment of the new methodology

An important feature of the new method is that the hazard degree is determined by evaluating which is the worst hazard condition among *all* those affecting a given point. This means that the worst condition found at the point examined may not necessarily correspond to that of highest intensity, according to the structure of the intensity–frequency diagram used. Figure 13 illustrates this aspect, with reference to the application at Creux de Chippis already analysed, and shows how hazard curves also constitute a helpful tool for quickly visualising:

- The evolution of the hazard degree along the slope (Fig. 13, top), i.e. each curve is referred to a different slope unit (abscissa x), for a given rock fall return period value T_f.
- The evolution of the hazard when a change in the rock fall failure time T_f occurs (Fig. 13, bottom), which gives an idea about the way hazard changes at a given location of the slope, should the frequency of failure scenario change.

Referring to the cyan curve in the top diagram of Fig. 13 (x= 405 m), as well as to the cyan curve in the bottom diagram (for T_f= 30 years·m), it is quite evident that blocks characterised by low energies and low return periods may yield a higher hazard degree than blocks reaching the same point with higher energies but higher return periods. In the former situation, some E_i–T_i couples are located in the moderate hazard domain of the diagram, while the points representing the latter situation are in the low hazard domain. This example clearly illustrates that a given degree of hazard is the result of the combination of the two parameters.

Additionally, the new Cadanav keeps some important advantages of the previous version of the methodology (Abbruzzese et al. 2009).

First, it is quite insensitive to the extreme propagation of one block (or just a few) as obtained from rock fall simulation. Actually, in the new procedure the highest $P(E,x)$ values are associated to the highest energy values at each abscissa, which means that the highest energies are associated in turn to the lowest $P_r(E,x)$ values, and therefore to the highest return periods $T(E,x)$. These $T(E,x)$ values associated to "extreme" conditions are located outside the intensity–frequency diagram, i.e. $T(E,x)>300$ years and therefore have no influence on zoning.

In relation to this point, the new Cadanav methodology is also not highly sensitive to the number of runs performed in a trajectory simulation. As done for the original procedure, comparisons were carried out at several sites between the zoning obtained from 300 and 10,000 trajectory data sets, for different block volumes and return periods. As it happens for the original approach, noticeable changes in zoning can be observed only when the raw results obtained from the 300 and the 10,000 runs simulations present some marked dissimilarities due to the stochastic character of the computations.

Zoning issues linked to the structure of the Swiss diagram

One point which is worth discussing separately from methodological aspects concerns the shape of the Swiss intensity–frequency diagram, as this also conditions hazard zoning.

In particular, as observed in the previous section (Figs. 11 and 12), the moderate hazard zone can disappear according to original Cadanav. More in detail, what happens in these cases is that the limit of this zone is indeed predicted by the original procedure, but its location is in fact

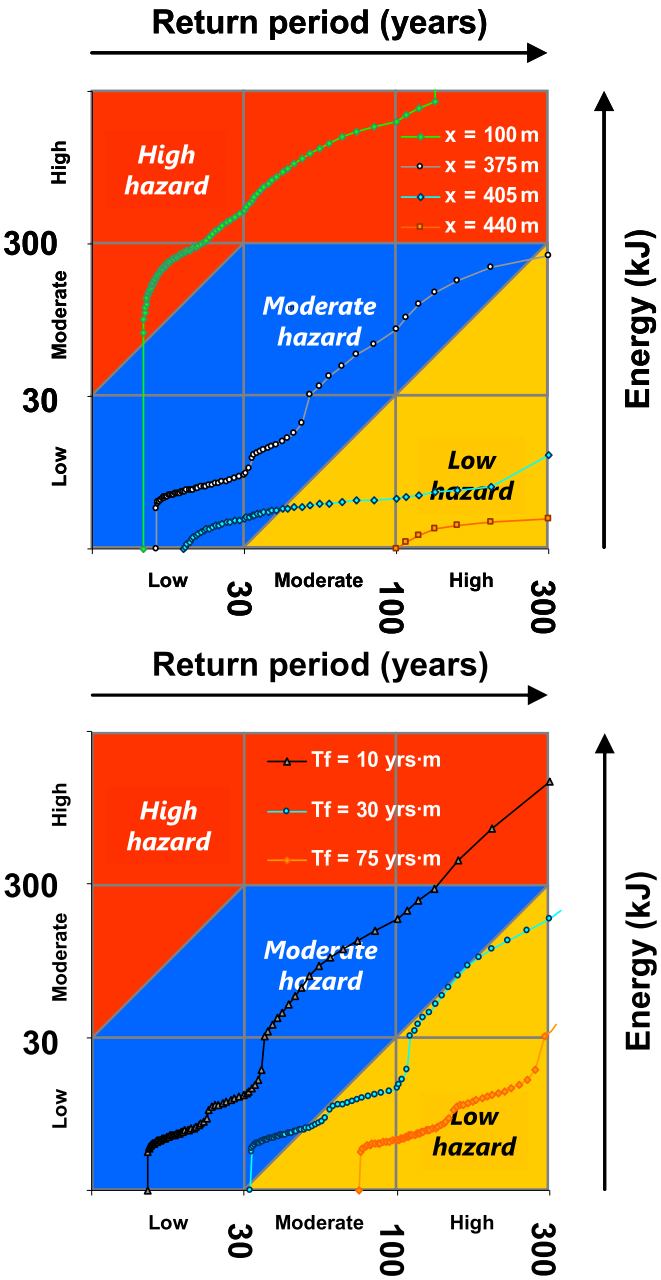

Fig. 13 Information provided by hazard curves once superimposed on an intensity–frequency diagram. *Top* evolution of hazard at different abscissas along the slope (T_f=10 years·m). *Bottom* evolution of hazard at a given abscissa for different return period scenarios (x=360 m)

the same as the high hazard zone limit. This problem is due to the "triple point" of the Swiss diagram, point 7 (E=300 kJ, T=300 years), where all the three hazard domains converge. When the condition yielding the extent of the moderate hazard zone is given by point 7, moderate and high hazard zone limits overlap (because this point yields both limits) and, as the most unfavourable condition must be selected for zoning, the moderate zone vanishes.

Similarly, the peculiar shape of the Swiss intensity–frequency diagram may generate missing moderate hazard zones also in the new Cadanav methodology. Indeed, the new procedure does not

provide any moderate hazard zone when the change in the degree of hazard is controlled by energy–return period couples located near the triple point. Figure 14 shows two hazard curves, referred to abscissas located in proximity of the one where the change from high to low hazard occurs. Passing from x=356 m (grey curve) to x=360 m (cyan curve), the intermediate situation of having some curves crossing only the moderate and low hazard domains is not encountered, which means that no moderate hazard zone is predicted.

New Cadanav versus other available methodologies

The new Cadanav methodology constitutes a more rigorous and detailed approach to hazard assessment and zoning compared to its original version, but also to other existing procedures.

In this respect, first of all, the new methodology is fully quantitative, in contrast with several others, starting from the definition of the failure frequency, up to the hazard assessment techniques used.

Regarding the consideration of the time recurrence of the events, some methodologies tackle this point qualitatively (Rouiller et al. 1998; MATE/METL 1999; Copons 2007), while other approaches do not directly consider or do not consider at all this parameter (Mazzoccola and Sciesa 2000; Crosta and Agliardi 2003; Lan et al. 2007).

When rock fall inventories are missing for quantifying the rock fall frequency, as this is frequently the case, the new Cadanav methodology could still be considered for the delineation of hazard zones. Based on a detailed study and characterisation of the cliff, a susceptibility of failure can be assigned to the potential departure zones (e.g. Rouiller et al. 1998; Mazzoccola and Sciesa 2000; Mölk et al. 2008). If a correspondence is then assumed between the susceptibility of failure and the time recurrence of the events, the new Cadanav methodology can be applied. For instance, according to the Swiss guidelines, return periods of 1, 30 or 100 years could be associated with high, moderate or low susceptibilities of failure, respectively. However, as the uncertainties about the time recurrence of the events significantly affect the hazard zoning results (Figs. 11 and 12), it is advisable to consider various failure scenarios.

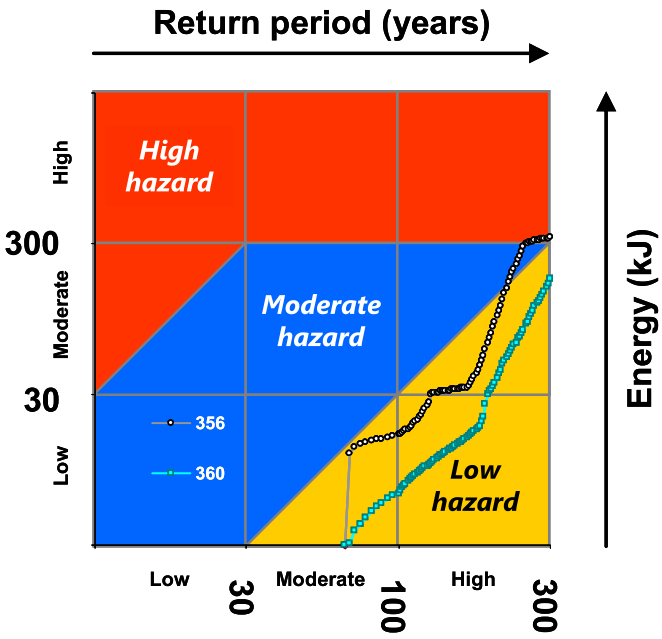

Fig. 14 Example of discontinuous transition from high to low hazard directly

For what concerns the post-processing of trajectory modelling data, the new Cadanav methodology is free from subjective assumptions about the energy which is relevant to consider for hazard zoning. With respect to other methodologies, all the energy values are considered at every point of the slope, with their associated probability, which does not require to define a single representative value of energy at each point, e.g. maximum (Crosta and Agliardi 2003; Lan et al. 2007; Copons 2007) or n^{th} percentile-based, or other processing (Jaboyedoff et al. 2005). The new Cadanav methodology makes also the selection of appropriate thresholds for classifying the probability of reach unnecessary, contrary to other approaches (Rouiller et al. 1998; Mazzoccola and Sciesa 2000; Desvarreux 2007; Copons 2007).

Additionally, the combination of energy and return period by means of the hazard curves is rigorous and constitutes a real coupling of these parameters, rather than a simple superimposition of e.g. the envelope of maximum energy values (or other percentile-based envelope) with probabilities of reach that do not necessarily correspond to these energies (Rouiller et al. 1998).

Finally, whereas the hazard zoning performed with some methodologies (Rouiller et al. 1998; Desvarreux 2007; Copons 2007) may be highly conditioned by the number of runs performed in a trajectory simulation and by the presence of possible outliers in the results (Abbruzzese et al. 2009), the new Cadanav methodology, as its original version, is characterised by a very low sensitivity with regards to these issues.

Wide applicability of the methodology

Despite new Cadanav was applied following the matrix diagram contained in the Swiss Codes all throughout this paper, the new procedure is in fact applicable regardless of the intensity–frequency diagram used. The construction of the hazard curves does not depend on the diagram, as the curves are simply superimposed to it. Thus the methodology could be applied also if the structure and/or threshold values of the matrix would change (e.g. for applications according to recommendations of other countries in which different diagrams are used).

Finally, even though the analyses presented in this paper always dealt with diffuse instability problems affecting linear cliffs, which can therefore be studied along 2D slope profiles, the implementation of the new Cadanav methodology is general and flexible (Abbruzzese and Labiouse, in preparation). In particular, it not only allows for evaluating rock fall hazard for complex scenarios involving several sources and event return periods, but it can also be applied for performing hazard zoning for 3D topographies, starting from 3D trajectory modelling results.

Conclusions

A new procedure for rock fall hazard assessment and zoning at the local scale was presented in this paper: the new Cadanav methodology. Starting from available information on rock fall failure frequency and trajectory simulation results, this approach to hazard zoning combines energy–return period curves (hazard curves) with the use of intensity–frequency diagrams.

The new procedure is fully quantitative and introduces several improvements to hazard zoning, especially for what concerns the use of trajectory modelling results and the technique applied for evaluating the hazard.

Hazard curves are meant to provide a complete view of all the hazard scenarios potentially affecting a given site, and constitute a useful tool for effectively visualising the hazard evolution along the slope. As this technique is free from the assumptions characterising an original version, it can provide a correct hazard assessment and zoning for both regular and complex topographies, including also those situations where the original methodology was not satisfactory (i.e. irregular slope profiles). At the same time, the new procedure keeps the advantages of the original approach, i.e. it is not highly sensitive to the number of trajectories performed in a simulation, and quite insensitive to the extreme results obtained from a simulation (longer propagation path of one or a few blocks).

More in general, when compared to other existing methodologies, the new Cadanav procedure proves to be rigorous and robust in terms of hazard assessment. It performs well in all the conditions tested and provides a more objective zoning, which proves to be completely independent of the user.

Acknowledgements

This work is based on a PhD thesis completed in the framework of the Marie Curie Research Training Network "Mountain Risks: from prediction to management and governance" (6th Framework Program of the European Commission). The authors would like to thank the European Commission for supporting the research project.

They would also like to thank the authorities of the Canton of Valais, for authorising the hazard analyses for the sites studied, and Jean-Bruno Pasquier at the Bureau Géoval, for performing the rock fall trajectory simulations.

References

Abbruzzese JM (2011) Improved methodology for rock fall hazard zoning at the local scale, PhD Dissertation, École Polytechnique Fédérale de Lausanne (EPFL)

Abbruzzese JM, Sauthier C, Labiouse V (2009) Considerations on Swiss methodologies for rock fall hazard mapping based on trajectory modelling. Nat Hazard Earth Syst Sci 9:1095–1109

Altimir J, Copons R, Amigó J, Corominas J, Torrebadella J, Vilaplana JM (2001) Zonificació del territori segons el grau de perillositat d'esllavissades al Principat d'Andorra. La Gestió dels Riscos Naturals, 1es Jornades del CRECIT (Centre de Recerca en Ciencies de la Terra), Andorra la Vella, 13–14 September 2001, 119–132

BLfU (Bayerisches Landesamt für Umwelt) (2007) Maßnahme 3.2a "Schaffung geologischer und hydrologischer Informationsgrundlagen", Vorhaben "Gefahrenhinweiskarte Oberallgäu", Bayerisches Landesamt für Umwelt, internal press

Chau KT, Wong RHC, Liu J, Lee CF (2003) Rockfall hazard analysis for Hong Kong based on rockfall inventory. Rock Mech Rock Eng 36(5):383–408

Copons R (2007) Avaluació de la perillositat de caigudes de blocs rocosos al Solà d'Andorra la Vella. Andorran Research Centre Press, St. Julià de Lòria-Principality of Andorra

Corominas J, Copons R, Moya J, Vilaplana JM, Altimir J, Amigó J (2005) Quantitative assessment of the residual risk in a rock fall protected area. Landslides 2:343–357

Crosta GB, Agliardi F (2003) A methodology for physically based rockfall hazard assessment. Nat Hazard Earth Syst Sci 3:407–422

Desvarreux P (2007) Problèmes posés par le zonage. Lecture notes from the course Université Européenne d'été 2007: éboulements, chutes de blocs—rôle de la forêt, Courmayeur, September 2007

Dussauge-Peisser C, Helmstetter A, Grasso JR, Hantz D, Desvarreux P, Jeannin M, Giraud A (2002) Probabilistic approach to rock fall hazard assessment: potential of historical data analysis. Nat Hazards Earth Syst Sci 2:1–13

Einstein H, Sousa R, Karam K, Manzella I, Kveldsvik V (2010) Rock slopes from mechanics to decision making. In: Rock mechanics in civil and environmental engineering—proceedings of the European Rock Mechanics Symposium (EUROCK) 2010, Lausanne, Switzerland.

Fell R, Ho KKS, Lacasse S, Leroi E (2005) A framework for landslide risk assessment and management. In: Hungr O, Fell R, Couture R, Eberhardt E (eds) Landslide risk management. Taylor and Francis Group, London, pp 3–25

Fell R, Corominas J, Bonnard C, Cascini L, Leroi E, Savage WZ, on behalf of the JTC-1 Joint Technical Committee on Landslides and Engineered Slopes (2008) Guidelines for landslide susceptibility, hazard and risk zoning for land use planning. Eng Geol 102:85–98

Guzzetti F, Crosta G (2001) Logiciel STONE/Programma STONE. Interreg IIc: Prévention des mouvements de versants et des instabilités de falaises: confrontation des méthodes d'étude d'éboulements rocheux dans l'arc Alpin, Interreg Communauté européenne, pp 206–211

Hantz D (2011) Quantitative assessment of diffuse rock fall hazard along a cliff foot. Nat Hazard Earth Syst Sci 11:1303–1309

Hantz D, Vengeon JM, Dussauge-Peisser C (2003) An historical, geomechanical and probabilistic approach to rock fall hazard assessment. Nat Hazards Earth Syst Sci 3:693–701

Hungr O, Evans SG, Hazzard J (1999) Magnitude and frequency of rock falls along the main transportation corridors of southwestern British Columbia. Can Geotech J 36:224–238

Jaboyedoff M, Dudt JP, Labiouse V (2005) An attempt to refine rockfall hazard zoning based on the kinetic energy, frequency and fragmentation degree. Nat Hazard Earth Syst Sci 5:621–632

LCPC - Laboratoire Central des Ponts et Chaussées (2004) Les études spécifiques d'aléa lié aux éboulements rocheux – Guide technique, Collection environment: les risques naturels, 86 pp

Labiouse V, Abbruzzese JM (2011) Rockfall hazard zoning for land use planning. In: Nicot F, Lambert S (eds) Rockfall engineering. Wiley, New York, pp 211–253

Lan H, Derek Martin C, Lim HC (2007) Rockfall analyst: a GIS extension for three-dimensional and spatially distributed rockfall hazard modelling. Comput Geosci 33:262–279

Lateltin O, Haemmig C, Raetzo H, Bonnard C (2005) Landslide risk management in Switzerland. Landslides 2:313–320

MATE/METL (1999) Plans de prévention des risques naturels (PPR), Risques de mouvements de terrain, Guide méthodologique, La documentation Française

Mazzoccola D, Hudson J (1996) A comprehensive method of rock mass characterization for indicating natural slope instability. Q J Eng Geol Hydrogeol 29:37–56

Mazzoccola D, Sciesa E (2000) Implementation and comparison of different methods for rockfall hazard assessment in the Italian Alps. in: Landslides in Theory, Research and Practice, Proceedings of the 8th International Symposium on Landslides, Vol 2, edited by Thomas Telford, 1035–1040

Mölk M, Poisel R, Weilbold J, Angerer H (2008) Rockfall rating systems: is there a comprehensive method for hazard zoning in populated areas?. In: Proceedings of the 11th Interpraevent 2008 Congress, Vol 2, 26–30 May 2008, Dornbirn (Vorarlberg), Austria

Raetzo H, Lateltin O, Bollinger D, Tripet JP (2002) Hazard assessment in Switzerland—codes of practice for mass movements. Bull Eng Geol Environ 61:263–268

MR (Mountain Risks Research Training Network) (2010) Glossary: http://www.unicaen.fr/mountainrisks/spip/spip.php?page=presentation_article&id_article=51#1, accessed 15 September 2010

Rouiller JD, Jaboyedoff M, Marro C, Phillippossian F, Mamin M (1998) Pentes instables dans le Pennique valaisan, Rapport final PNR 31, VDF Zürich

Spang RM, Krauter E (2001) Rockfall simulation—a state of the art tool for risk assessment and dimensioning of rockfall barriers. In: Kühne M et al (eds) International Conference on Landslides—causes, impacts and countermeasures. United Foundation Engineering, Davos, pp 607–613

Volkwein A, Schellenberg K, Labiouse V, Agliardi F, Berger F, Bourrier F, Dorren LKA, Gerber W, Jaboyedoff M (2011) Rockfall characterisation and structural protection—a review. Nat Hazard Earth Syst Sci 11:2617–2651

J. M. Abbruzzese (✉) · V. Labiouse
School of Architecture, Civil and Environmental Engineering (ENAC),
Laboratory for Rock Mechanics (LMR),
Ecole Polytechnique Fédérale de Lausanne (EPFL),
EPFL-ENAC-LMR, Station 18, 1015 Lausanne, Switzerland
e-mail: jacopo.abbruzzese@epfl.ch
URL: http://people.epfl.ch/jacopo.abbruzzese